3D STRUCTURE OF DENSITY FLUCTUATIONS IN THE T-10 TOKAMAK AND NEW APPROACH FOR CURRENT PROFILE ESTIMATION

V.A. VERSHKOV, M.A. BULDAKOV, G.F. SUBBOTIN, D.A. SHELUKHIN, A.V. MELNIKOV, L.G. ELISEEV, P.O. KHABANOV, M.A. DRABINSKIY, N.K. KHARCHEV, D.S. SERGEEV, T.B. MYALTON, V.M. TRUKHIN, A.V. GORSHKOV, I.S. BELBAS, G.M. ASADULIN
National Research Center "Kurchatov Institute"
Moscow, Russian Federation
Email: V.vershkov@fc.iterru.ru

Abstract

Previous investigations of small-scale density fluctuation by means of correlation reflectometry in T-10 tokamak revealed the existence of several density fluctuation types and strong radial and poloidal variation of their amplitudes and correlation properties. This paper is focused on the new measurements of the 3D spatial distributions of the amplitudes, the radial correlation lengths and the long range correlations along the field lines for the different turbulence types. The properties of the density fluctuations were systematically studied with the improved reflectometers, data analyzing and acquisition hardware. The density fluctuations were measured by heterodyne correlation reflectometry using ordinary mode. New T-10 antenna set have horn antennae arrays at four places distributed toroidally and poloidally over tokamak torus. The experiments confirmed previously found strong poloidal amplitude asymmetry of the broad band and the quasi-coherent oscillations and the uniform poloidal distribution of stochastic low frequency fluctuations. The presence of those turbulence types was also proved by the measurements of perturbation properties using heavy ion beam probe diagnostic. The radial correlation measurements were performed at four poloidal angles to understand the poloidal dependence of the radial correlation length for the different fluctuation types. The significant decrease of the radial correlation lengths towards the high magnetic field side was observed for quasi-coherent and stochastic low frequency turbulence types. The long range correlations along the field lines were measured by the reflectometers in two cross-section separated by 1/4 of the torus. The reflectometers have the same frequency thus provide reflection from the same magnetic surface. Reflection radii are chosen by the frequency variation of the launched wave from shot to shot in a series of reproducible discharges. The measurements were carried out at the low and the high magnetic field side with two currents and simultaneous reverse of the direction of the toroidal magnetic field and the plasma current. Resonance radii were also calculated using 3D tracing of the magnetic field line and demonstrate good agreement with experiments. These results allow to propose the new approach for the current profile measurements in tokamaks.

1. INTRODUCTION

The paper continues the series of previous publication devoted to the investigations of small-scale density fluctuation characteristics [1-4] and expands previous results with the new experimental material. The main goals of the paper were the confirmation of the different turbulence types and complete characterization of their properties. Such characterization includes the radial and poloidal spatial distributions of the fluctuations amplitudes, the radial correlation measurements at several poloidal angles and the longitudinal propagation of different fluctuation types along the magnetic field line by means of Long Range Correlations (LRC).

2. EXPERIMENTAL SETUP

Small scale density fluctuations were measured using ordinary mode correlation reflectometry [1] with new T-10 antenna set and 5 channel Heavy Ion Beam Probe diagnostic (HIBP) [5]. The 5 channel HIBP measured plasma density and potential fluctuations at 5 adjacent points along the beam pass at Low Magnetic Field Side (LFS) equatorial area of tokamak [6]. The positions of reflectometry antennas and HIBP are shown schematically in Fig. 1. The new T-10 antenna set had antenna arrays at four positions distributed toroidally and poloidally over the T-10 tokamak. The antenna arrays were positioned at poloidal angles 0, 60, 120 and 180° (counting

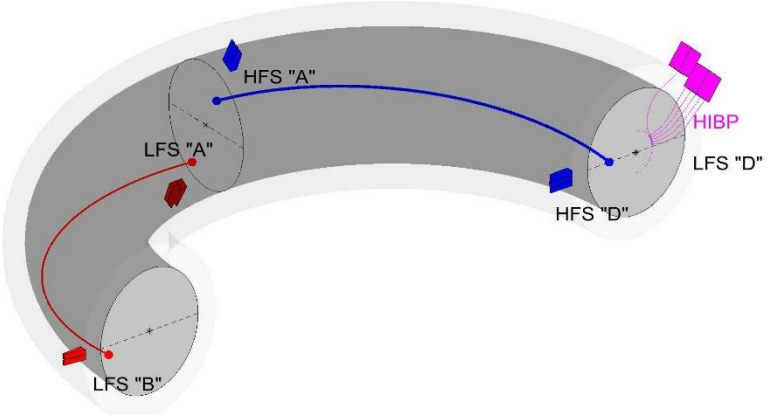

FIG. 1. The schematics of the T-10 reflectometry and HIBP diagnostics.

from LFS equatorial plane) and allowed to investigate the radial distribution of the fluctuation amplitudes for each poloidal angle. The probing radius was chosen by the change of the launched frequencies in the range from 40 to 60 GHz in a series of reproducible discharges. All antenna arrays, except LFS equator, had several horns to measure the correlations at two poloidal points. It gives information about the poloidal correlation and the poloidal velocities of the fluctuations. Two independent heterodyne reflectometry systems were based on the semiconductor voltage-controlled microwave generators and were used for the radial correlation measurements. They share the same transmission line and antennae. The frequencies of both generators were measured by spectral analyzer and were set before each discharge with an accuracy of 1 MHz. The antenna arrays were distributed along the torus in order to enable measurements of LRC at ¼ of the torus at LFS and High Magnetic Field Side (HFS) as it is shown by curves connected observation points in Fig.1. Two reflectometers were set at the close frequencies, which provide reflection from the same magnetic surface and probed plasma at both ends of the field line in a series of reproducible discharges with variation of the probing frequency. The goal of such a measurements was to investigate the correlation properties of the fluctuations along the field line. The principle of an experiment illustrated in a Fig.2. Let us treat the situation when a perturbation had the constant phase along the magnetic field line. The middle situation (red one) corresponds to the case when the reflection spots of the beams 1 and 2 lay at the same magnetic line and thus correlation function delay should be zero. If the reflection point shifts towards plasma periphery where field line pitch angle is lower magnetic field line footprint from reflection spot 1 moved from reflection spot 2. Observed coherency maximum in this case will have some negative delay due to the poloidal rotation. If the reflection spot shift towards center from resonance position the positive delay will be observed. The delay value is equal to the ratio of the shift of magnetic field line due to the magnetic shear and the poloidal velocity. Since the poloidal velocity could be measured using the poloidal antenna array (beams 3 and 4), one could determine also the local magnetic shear.

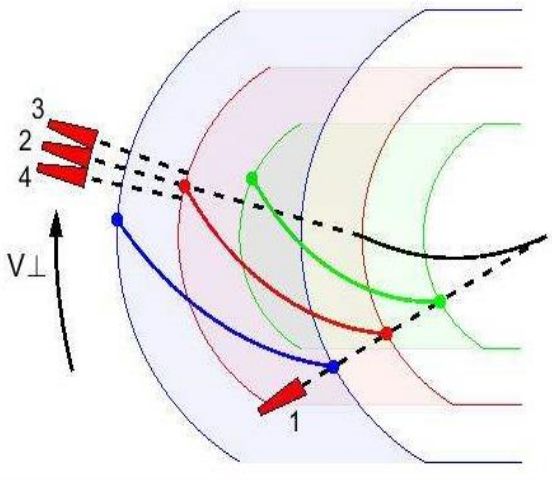

FIG. 2. The schematics of LRC by means of change of reflection radius.

Alternative approach utilizes measurements at the one fixed frequency shown schematically in Fig.3. Several receiving antennae provide information from two poloidally separated spots. Thus the simultaneous measurements with four different toroidal inclination of the probing lines became possible (α_1-α_4 in Fig3). LRC delay of the signals was measured for each antennae combination. One can expect the linear variation of the measured delay of LRC with the tilt angle between reflection points. So it is possible to extrapolate four measured values of LRC delays to zero delay and find the inclination of the magnetic field line at the cutoff radius. The example of such a measurement for quasi-coherent fluctuations (QC) shown in Fig. 4. The resonant poloidal transform at ¼ of the torus should be reached at 83º (Fig.4a), which may correspond to q=1.085. But as the inclination of the field line was measured locally at HFS, so corresponding *q* value should be found taking into account the real magnetic configuration. The situation will be more complex in case of the finite propagation velocity along the field line or propagation of the perturbations at the angle to the field line. Thus LRC experiments includes search for the evidence of the fluctuation propagation with finite velocity or/and the propagation at some angle to the field line.

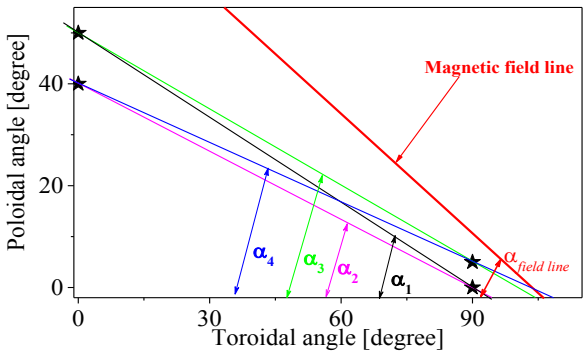

FIG. 3. The schematics of LRC at one reflection radius, with combinations of antennas at HFS (shown by stars).

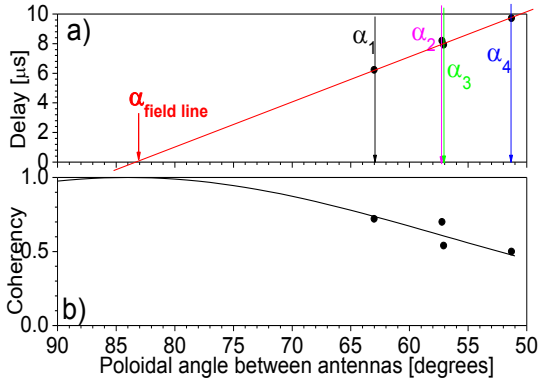

FIG. 4. Example of alternative approach of LRC at HFS for LFQC modes in case of central reflection

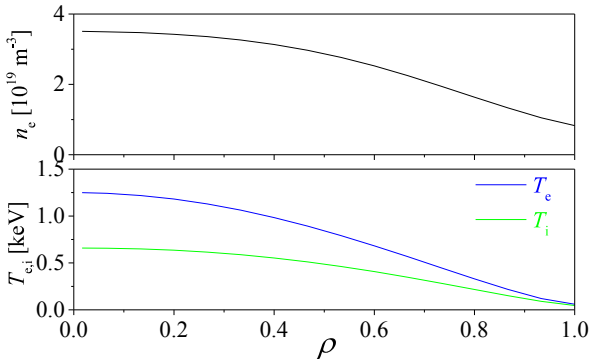

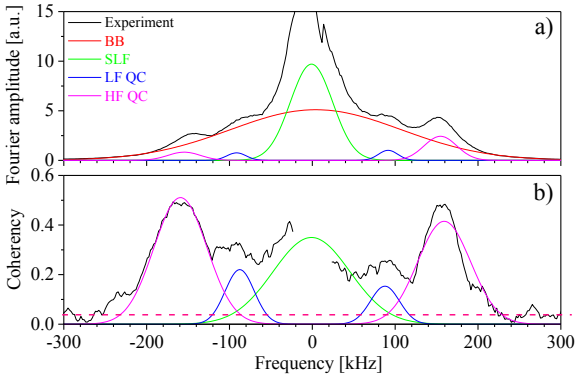

FIG. 5 Electron, ion temperatures and density profiles. *FIG. 6. Example of Spectrum decomposition on fluctuation types*

The measurements were carried out mainly in ohmic discharges (except where noted) in T-10 tokamak with major and minor radii R = 1.5 m and a = 0.3 m correspondingly. The discharge parameters were I_p = 220 - 250 kA, B_T = 2.4 T and n_e = 1.7 - 3·10^{19} m^{-3}. Typical profiles of electron and ion temperatures and electron density are shown in Fig. 5. The density profile was measured with 16 channels interferometer. Electron temperature profiles were measured with Electron Cyclotron Emission radiometry (ECE), soft X-ray radiation spectra analyzer (SXR) and laser scattering techniques. Ion temperature profile and impurity concentration were measured with charge-exchange recombination spectroscopy (CXRS). Z_{eff} was measured via continuum light intensity in visible band.

3. RESULTS

New results are based on previous classification of the fluctuations that identified three main turbulence types [2] shown in the Fig. 6.a,b. They include Broad Band (BB), Stochastic Low Frequencies (SLF) and the High and Low Frequency Quasi-Coherent fluctuations (HFQC and LFQC). The experimental spectrum can be decomposed into the sum of four spectra for each turbulence type, as shown in Fig.6,a,b.

3.1. Broad Band

Broad Band has wide and smooth spectrum that spreads from zero frequency up to 300-500 kHz. These fluctuations have the low spatial coherency. The typical autocorrelation function of the non-filtered reflectometry signal received by antennae at 120º poloidal angle is shown in Fig. 7a. BB and SLF turbulence types dominate in the signal in this case. So autocorrelation function can be decomposed into two components. The autocorrelation time for BB fluctuations appeared to be 2.7 μs. Taking into account the measured poloidal velocity for QC fluctuations 3.5×10^5 cm/s it gives the poloidal dimension of BB fluctuation about 1 cm. It can be seen in Fig. 6b that the BB component practically not correlated if signals are received from two antenna separated poloidally at 0.1 rad. Thus the typical life time of the BB fluctuations should be less or about 2.5 μs, which is in good agreement with one found from autocorrelation time. The BB component gives the major input to the total level of the density perturbation. It was found that the radial profile of the relative density fluctuations of BB in T-10 can be described as $\delta n/n_e = 0.2 q_a \cdot r/L_n$, where r is the minor radius, $L_n = (\partial \ln n_e / \partial \ln r)^{-1}$ is density profile length, q_a is the safety factor at the boundary; the multiplier 0.2 was chosen to meet the experimental data [7].

The radial correlation measurements were made at four poloidal angles for the first time (Fig. 8). The

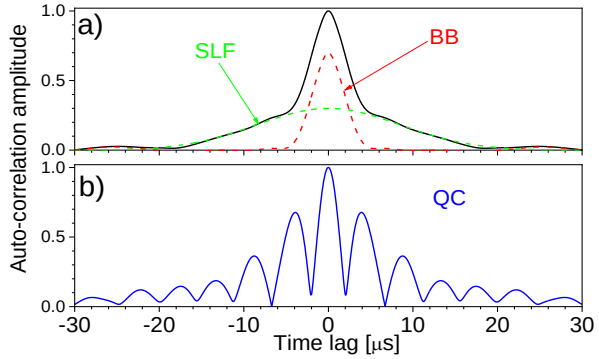

FIG. 7 Auto-correlation functions of BB and QC.

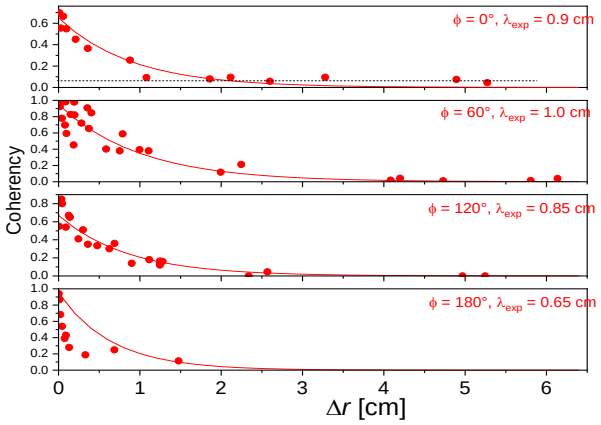

FIG. 8. Radial correlations for BB at 4 poloidal angles.

values of the BB correlation were characterized by the coherency between two radially separated reflectometry signals in the frequency range 250 – 350 kHz, where the QC fluctuations input was negligible. The correlation length slightly decreases from LFS towards HFS yet remains close to 0.9 cm. The phase shift between the signals was found to be zero at all radial separations. It is important to mention that correlations exponentially decay up to noise level without the long tails which are predicted by theory [8]. It means that the radial structure of the BB perturbations may have oscillating feature [4]. It is also seen that at HFS equator correlations steeply decrease with a decay length about 0.1 cm, but after that restored to the overall decay length of 0.65 cm in agreement with previous measurements [4]. Although it is possible to consider observed anomalous behavior as turbulence peculiarity at HFS, this hypothesis is inconsistent with the smooth correlation function at 120º. We attribute observed phenomena to the specific properties of the HFS antennae array.

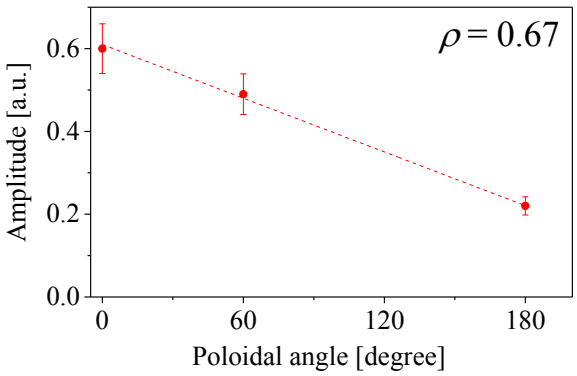

FIG. 9. Poloidal distribution of BB amplitude.

The poloidal distribution of the BB fluctuation amplitude at ρ = 0.67 is shown in Fig.9. One could see strong ballooning of the BB fluctuations amplitude. LRC measurements demonstrate that zero correlation for the BB fluctuation along the field line even at ¼ of the torus (2.4 m). So the BB fluctuations at each poloidal angle could be treated as independent pointing that BB is generated locally. The measured poloidal asymmetry of the fluctuation amplitude could be explained by the asymmetry of the BB drive.

3.2. Quasi-coherent fluctuations

Quasi-coherent fluctuations were originally found by correlation reflectometry in T-10 experiment [9]. Later these fluctuations were also observed at TEXTOR [10], FTU [11], Tore Supra [12], JET [13] and ASDEX-U [14]. LFQC were also observed in T-10 with the single-channel Heavy Ion Beam Probe (HIBP) diagnostic [15].

Low and High frequency quasi-coherent modes observed as two smooth maxima typically at 120 and 200 kHz in turbulence spectrum in T-10 experiments. Those values correspond to poloidal wavelength (at r = 20 cm with measured poloidal velocity 4×10^5 cm/s) 3.3 and 2 cm and $k_{pol}\times\rho_i$ equals to 0.16 and 0.27 respectively. $k_{pol}\times\rho_i$ values are in a good agreement with the previous results, where it was shown that such values at r = 20 cm correspond to the core values 0.3 and 0.7 respectively. HFQC was observed at radii between 15 and 25 cm, were trapped particles have maximal concentration. In contrast LFQC is observed for the central and periphery regions. These properties are typical for Trapped Electron Mode (TEM) and Ion Temperature Gradient (ITG) instabilities respectively [2,3].

HIBP capabilities were expanded in new experiments to measure density and potential at five close spatial points simultaneously thus providing the possibility of correlation measurements [6]. The results of correlation measurements between poloidally separated volumes at ρ = 0.67 are shown in Fig.10. It is clearly seen LFQC peak in amplitude and coherency spectra at 80 kHz and SLF maxima below 20 kHz. BB fluctuation was not

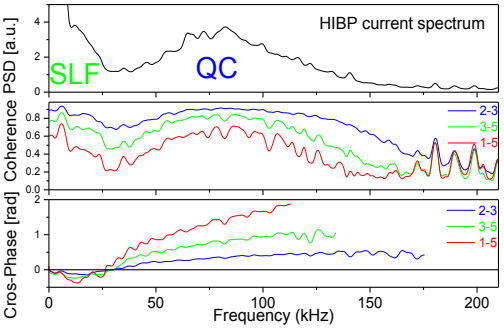

FIG. 10. HIBP correlations for density oscillations, measured with four slits. Top-power spectrum of the first channel; middle - coherency; bottom - cross-phase.

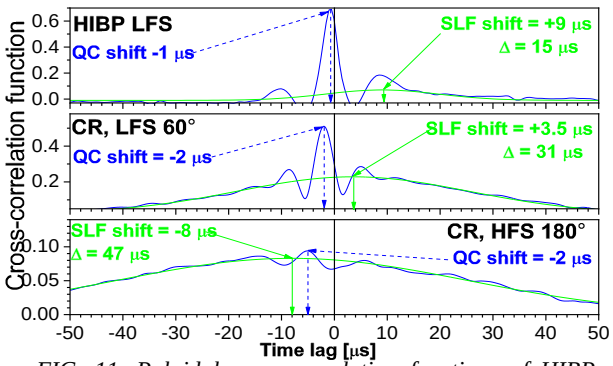

FIG. 11. Poloidal cross-correlation functions of HIBP (top) and reflectometry (middle) at LFS; Bottom-cross correlation of reflectometry at HFS.

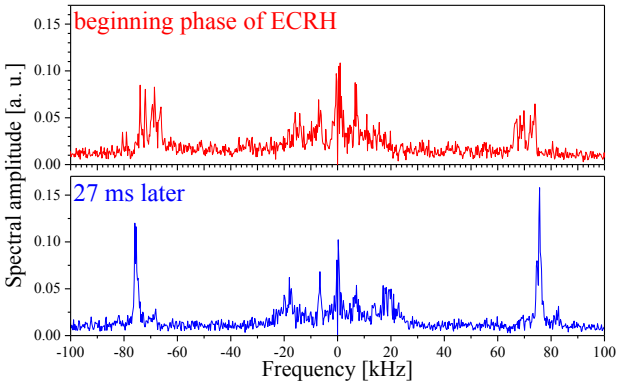

FIG. 12. Evolution of QC spectrum during off-axis ECRH

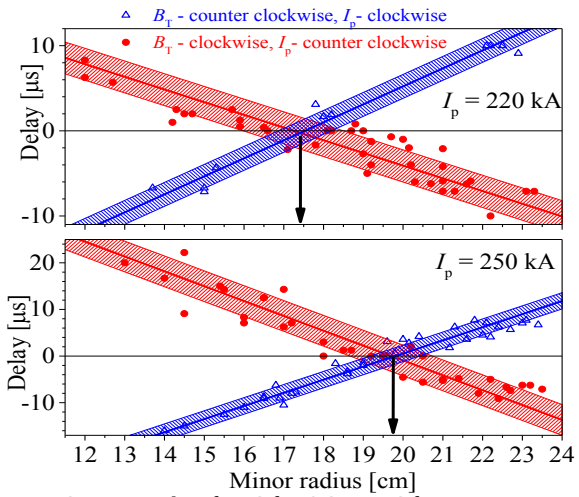

FIG. 13. Results of LRC for QC at LFS for two currents and reversal of the toroidal magnetic field and current

presented in the amplitude spectrum due to the spatial resolution of HIBP diagnostic that is about 1.5 cm in poloidal direction. One can also see that LFQC and SLF, besides separation in frequency spectra, have different direction of poloidal rotation (Fig.10 bottom). The opposite direction of LFQC and SLF rotation is supported by recent reflectometry cross-correlation (CR) measurements (Fig.11) and previous observations [3]. The QC and SLF maxima in cross-correlation function are shifted in opposite directions for both CR and HIBP at LFS. Above data could be a prove of the different origin of SLF and QC fluctuation types. Positions of the observation points for HIBP and reflectometry LFS allow to perform LRC between diagnostic data. Such correlations were observed in experiment for QC fluctuations.

Spectacular behavior of QC modes was observed in recent experiments with peripheral ECRH. Fig. 12 shows evolution of the turbulence spectra in plasma core during off-axis ECRH. Off-axis ECRH increase the temperature at plasma periphery and leads to flattening of the current profile that is manifesting in the disappearance of the sawtooth oscillations. Modification of current profile leads to the increase of the distance between rational surfaces with moderate m and n numbers. The upper spectrum is related to the beginning of ECRH and the bottom one is taken 27 ms later. One can see that wide initial peak of QC oscillations contracts to single mode structure. The measured angle velocity in these experiments was 2.5×10^4 rad/s thus gave poloidal m = 19. So it is possible to conclude that the QC oscillations origin is the excitation of the rational modes with high m numbers. The density of rational surfaces is high when magnetic shear has a high value so the QC oscillation peak is wide. If magnetic shear is low only a few mods can be exited. One can expect that the QC fluctuations should have the high correlations along the magnetic field lines if they arise due to the excitation of the rational modes. Such a LRC measurements were done at the LFS for two values of the plasma current. Correlation were measured between the reflectometry signals in two toroidally separated locations at LFS. The dependencies of delay times for the reflectometry signals versus the cutoff radii are plotted in Fig. 13 for LFQC fluctuations. The reflection radius was varied by the change of the probing frequency. Two series of discharges were investigated with the same parameters but reversed toroidal magnetic field and the plasma current. As both poloidal and toroidal fields were reversed simultaneously, the trace of the magnetic field line remains unchanged. Upper plot presents the LRC results for current 220 kA and bottom one presents the data for current 250 kA. The coherency values were rather high (0.2 - 0.3) thus proved the existence of the long correlation length along the field line for the QC fluctuations. Plots for both currents cross zero value at the same radial location. It is supposed that this resonance radius corresponds to the case when the reflection spots in both ports reach the same magnetic line. This evidence proves the hypothesis that the QC perturbations have a constant phase along the magnetic field line. One could see that the resonant radius is shifted outwards for the higher current because the resonant q value is shifted outwards also.

Radial correlation measurements were made at three poloidal angles: 0º, 60º and 120º (Fig.14). The amplitude of QC fluctuations was too small for measurements at HFS equator. Since the BB forms a background along the whole QC frequency band, it is difficult to separate their radial correlations when probing waves shares the same antennae and transmission lines. Poloidally shifted antennas were used to estimate the QC radial correlation to eliminate the BB interference. It was possible due to a zero poloidal coherency for the BB oscillations and high coherency for QC ones (Fig.6b). The same procedure was used in SLF radial correlation measurements. One can see that the coherency of QC oscillation remains constant up to the radial separation 5.5 cm at the LFS equatorial plane. The coherency at 60º begins to decrease with characteristic length 4 cm. The coherency function decays with the typical length 0.8 cm at 120º. The same strong decrease is seen on the plot of the QC amplitude versus

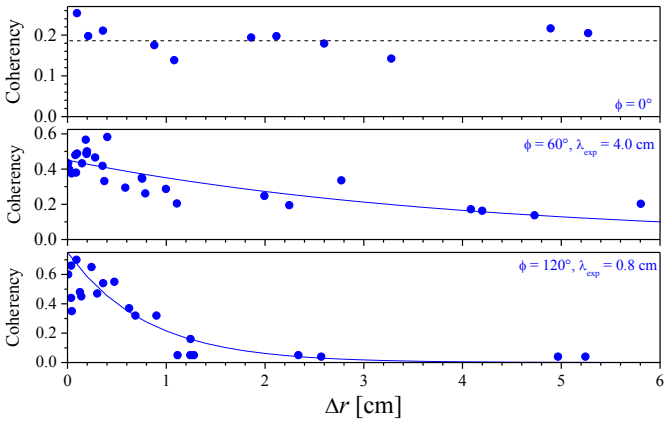

FIG. 14. Radial correlations for QC at 3 poloidal angles.

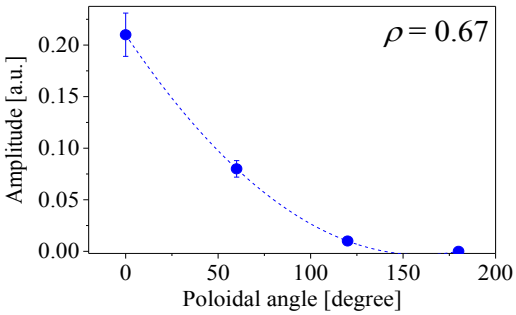

FIG. 15. Poloidal distribution of QC amplitude.

poloidal angle (Fig. 15). Strong decrease of QC amplitude at HFS is surprising taking into account high level of LRC along the magnetic line. Such results may be explained by the diagnostic peculiarities due to measurements non-locality [16]. Proposed hypothesis could explain the observation of LRC correlations for the QC fluctuations at HFS only in regions with low magnetic shear. The significant rise of the LFQC amplitude, poloidal coherency and LRC correlation at HFS are always observed when reflection occurs near q = 1 with flat current profile (Fig.4 - LRC and Fig.7b - QC autocorrelation). One can see that LRC correlation values for LFQC rise up to 0.7 (Fig.4b). The Gaussian extrapolation of poloidal coherency to the resonant value gives 38º, which corresponds to poloidal correlation length 6.5 cm (Fig. 4b). Special model was developed with perturbation transformation along the field line and 2D full wave reflection modelling [16]. It proved strong decrease of QC amplitude and correlation length at HFS due to distortion of QC oscillation in the presence of magnetic shear. It was found that QC fluctuations rotates in electron diamagnetic direction at all poloidal angles. The angular velocity Ω was about 2×10^4 rad/s, which is close to m/n = 2/1 MHD mode rotation.

3.3. Stochastic low frequency

SLF perturbation forms the bell-shape part of the spectrum in the low frequency range from 0 to 50-70 kHz. It is denoted “stochastic”, because they have smooth frequency spectrum in contrast to coherent modes in that frequency range arise due to MHD and GAM modes and often observed at frequencies below 30 kHz. The SLF fluctuations have high level of poloidal correlation. This turbulence type moves poloidally at LFS in ion diamagnetic direction, thus opposite to QC rotation (Fig. 10 and Fig. 11a,b). It changes movement direction at HFS to the electron diamagnetic direction, similar to QC (Fig.11c). The typical autocorrelation time varies from about 13 μs (Fig. 7a) up to 47 μs (Fig. 11b,c). An independent estimation of the SLF poloidal width can be made using LRC measurements. The LRC measurements for SLF fluctuations were performed using four antenna pairs at the HFS in discharge with off-axis ECRH (Fig. 16). One can see that maximum coherency value reached 0.8 value in such conditions. The antenna pair with the largest inclination was in resonant condition and had zero delay and the highest correlation value. The poloidal separation for the observation spots was 63 degrees and corresponded to q value about 1.43. The delay time increases with the fall of the inclination angle

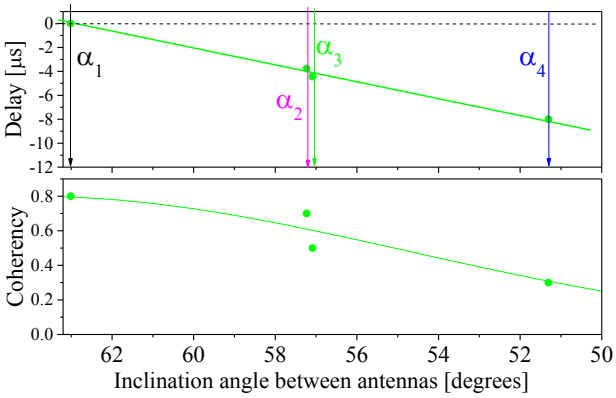

FIG. 16. LRC measurements for SLF at HFS with 4 antenna pair

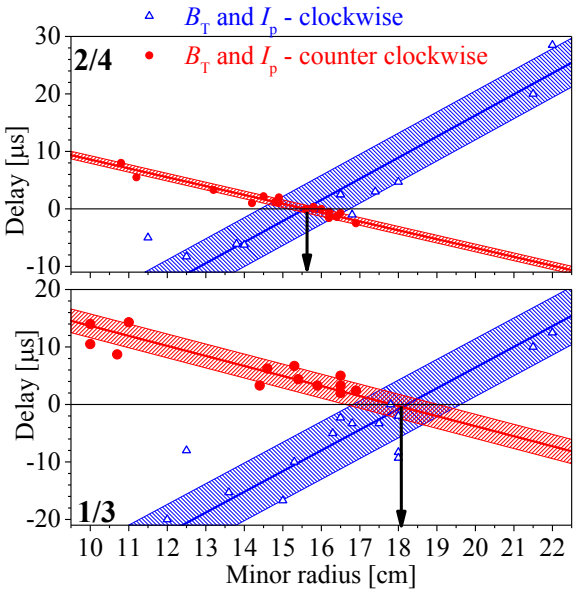

FIG. 17. LRC for SLF at HFS for two antenna pair and toroidal magnetic field and current reversal

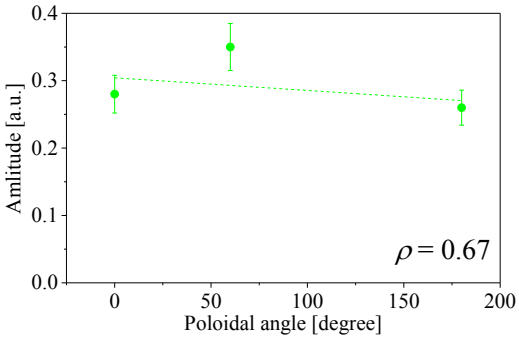

FIG. 18. Poloidal distribution of SLF amplitude.

and correlation amplitude decreases with typical scale about 13 degrees. It corresponds to the poloidal SLF width about 4.5 cm.

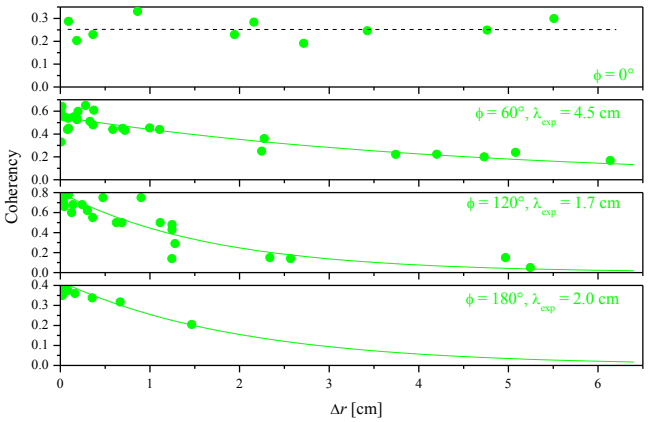

FIG. 19. Radial correlations for SLF at 4 poloidal angles.

The dependence of coherency delay versus probing radius for the SLF perturbations were estimated in LCR measurements at HFS (Fig. 17). The data corresponds to the correlation for antennae pairs with highest (top panel) and lowest (bottom panel) twisting angle between reflection spots. The results for different magnetic field orientation was obtained in the same way as for the QC LRC. The delay dependencies for both directions of the fields cross zero value at the same resonant radius. The resonant radius is bigger for the pair with lower twisting angle as it is expected. Thus SLF fluctuations also have long correlation length along the magnetic field line and may have constant amplitude similar to QC oscillation. The dependence of SLF amplitude on the poloidal angle is shown in Fig.18. One can see that in contrast to BB and QC, amplitude of SLF fluctuations is practically constant at all poloidal angles. This brings difficulties in LRC correlations of SLF at LFS, because SLF correlations is masked due to high level of the uncorrelated BB turbulence.

The results of the radial correlations of SLF at all four poloidal angles are presented in Fig.19. It is seen that SLF correlation practically is constant at LFS even at radial separation of 6 cm - similar to QC oscillations. The radial correlation length also decreases towards HFS yet remains sufficiently large at HFS equatorial plane. One should expect that radial correlation function for SLF fluctuation is affected by the magnetic shear due to long longitudinal correlation length and decrease of the radial correlation length at HFS is similar to the one observed for QC oscillation. But experiment did not reveal any delay of SLF in the radial correlation measurements. The physical origin of SLF remains unclear.

4. SUMMARY AND NEW APPROACH FOR THE CURRENT PROFILE ESTIMATION

Results of recent experiments with correlation reflectometry generally confirmed previously found classification of fluctuation types. The classification was confirmed for the first time by the correlation measurements with HIBP diagnostic. It was shown that BB fluctuations have the lowest poloidal, radial and toroidal correlation lengths. It was concluded that BB fluctuations generated locally. Observed poloidal asymmetry of their amplitude could be explained by the drive asymmetry. QC fluctuations have longitudinal correlation length that is significantly higher than 2.5 m. Some experiments point that such correlations were observed at 10 m [1]. Measurements of LRC with reverse of toroidal field and current support the hypothesis that QC fluctuations are constant along the field line. It was proposed that QC resulted from the excitation of the modes with high poloidal *m* number. The observed strong decrease of QC amplitude at the HFS in the region with the moderate magnetic shear can be an

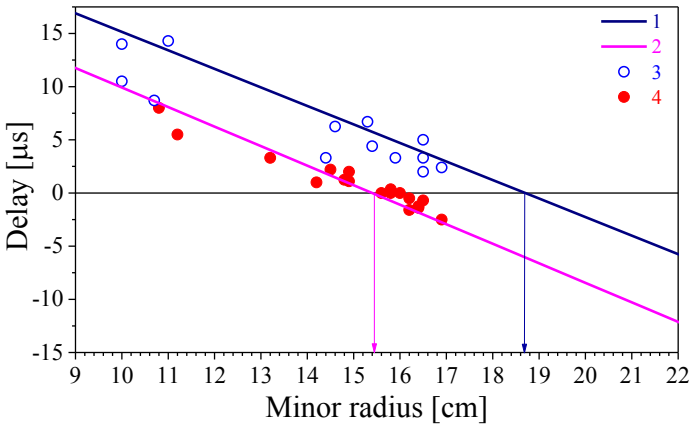

FIG. 20. Comparison LRC at HFS with model. 1 - modeling for antenna pair with low slope; 2 - modeling for antenna pair with high slope; 3 - experimental data for antenna pair with low slope; 4 - experimental data for antenna pair with high slope.

effect of reflectometry non-locality. The poloidal and radial dimensions of SLF were estimated. SLF fluctuations also have long correlation longitudinal length. New experiments demonstrate the opposite directions of SLF poloidal velocity at LFS with respect to QC fluctuations, while at HFS they move in one direction. Thus SLF moves in [B×∇B] direction both at LFS and HFS.

LRC experiments demonstrate that that QC and SLF fluctuations have long longitudinal correlation length and seems to have the constant phase along the magnetic field line. Thus such measurements can be used for current profile estimation. The LRC experimental results were compared with model, based on the calculated trace of magnetic field line, current density profile and measured fluctuation poloidal rotation in real antenna geometry (Fig. 20). The experimental results of two antenna pairs are presented and modelled in each case. One can see good coincidence between experimental and simulation data. The model reproduces both the resonant radii and the slope of the delays. It should be underlined that the physics of QC and SLF are not completely clear now. Besides that, QC and SLF oscillation could vanish at certain radii and poloidal angles. So it is proposed to use fluctuations with well-known physics. The most prominent candidate is Toroidal Alfven Eigen modes (TAE). But in difference to QC and SLF TAE modes have well defined radial locations. Thus the second LRC approach with several antenna pairs should be utilized. In this way reflectometry can measure all needed parameters: radial location of TAE by means density profile and spectral measurements, while the local magnetic transform by means of LRC.

ACKNOWLEDGEMENTS

The work was supported by Rosatom contract №1/15470-D/230/1040-18 . The research results, presented in section 3.2 and 3.3 obtained due to support by Russian Science Foundation project 14-22-00193.

REFERENCES

[1] Vershkov V.A., Soldatov S.V., Dreval V.V., A three-wave heterodyne correlation reflectometer developed in the T-10 tokamak, RSI **70**, 1700 (1999).
[2] M. Osipenko and T-10 Team. Transport and turbulence studies in the T-10 tokamak, Nucl. Fusion. **43** (2003) 1641–1652
[3] Vershkov V.A., Shelukhin D.A., Soldatov S.V., *et al.*, Summary of experimental core turbulence characteristics in ohmic and electron cyclotron resonance heated discharges in T-10 tokamak plasmas., Nucl. Fusion, 2005, **45** (10), S203-S226.
[4] Vershkov V.A., Andreev V.F., Borschegovskiy A.A., *et al*, Recent results of the T-10 tokamak, Nucl. Fusion **51** (2011) 094019
[5] Melnikov A.V., *et al.*, Heavy ion beam probing—diagnostics to study potential and turbulence in toroidal plasmas, Nucl. Fusion **57** (2017) 072004
[6] A.V. Melnikov, L.G. Eliseev, M.A. Drabinskij, *et al*, Electric potential and turbulence in OH and ECRH low-density plasmas in the T-10 tokamak, This conference, IAEA-CN-EX/P5-10
[7] V.A. Vershkov, D.A. Shelukhin, G.F. Subbotin, et al, Density fluctuations as an intrinsic mechanism of pressure profile formation, Nucl. Fusion **55** (2015) 063014 (15pp)
[8] E. Z. Gusakov and B. O. Yakovlev, Two-dimensional linear theory of radial correlation reflectometry diagnostics. Plasma Phys. Control. Fusion **44** (2002) 2525–2537
[9] V.A. Vershkov, S.V. Soldatov, D.A. Shelukhin, Dependence of core turbulence on the discharge parameters on T-10 and its correlation with transport, Proceedings of 16th Fusion Energy Conference 1996, IAEA-CN-64/A6-2 IAEA, Vienna, 1997, V 1, pp 519-533.
[10] A. Kramer-Flecken, V. Dreval, S. Soldatov, A. Rogister, *et al*, Turbulence studies with means of reflectometry at TEXTOR, Nucl. Fusion **44** (2004) 1143–1157
[11] V. A. Vershkov, D.A.Shelukhin, S.V.Soldatov, V.V.Chistiakov, Investigation of Core Turbulence Characteristics in Different Regimes in T-10 by Means of Correlation Reflectometry, Proc. 28 EPS Conf. Plasma Phys. Cont. Fusion, Funchal, 2001, V. **25A**, p. 1413.
[12] H. Arnichand, R. Sabot, S. Hacquin, *et al*, Quasi-coherent modes and electron-driven turbulence, Nucl. Fusion, **54** (2014), 123017
[13] H. Arnichand, R. Sabot, S. Hacquin, *et al*, Discriminating the trapped electron modes contribution in density fluctuation spectra, Nucl. Fusion, **55** (2015) 093021 (10pp)
[14] Prisiazhniuk D, Krämer-Flecken A, Conway G, *et al*. Application of poloidal correlation reflectometry to study turbulence at ASDEX-U, 12th Int. Reflectometry Workshop (FZ-Jülich, Germany), 2015
[15] Melnikov A.V., *et al.*, ECRH effect on the electric potential and turbulence in the TJ-II stellarator and T-10 tokamak plasmas, Plasma Phys. Control. Fusion **60** (2018) 084008
[16] V.A. Vershkov, D.V. Sarychev, G.E. Notkin, *et al*, Review of recent experiments on the T-10 tokamak with all metal wall, Nucl. Fusion **57** (2017) 102017 (15pp)